Electronic Supplementary Material (ESI) for Nanoscale.

Supplementary Materials

Supplementary Note 1 | Lorentz imaging at conditions for under-, in- and over-focus.

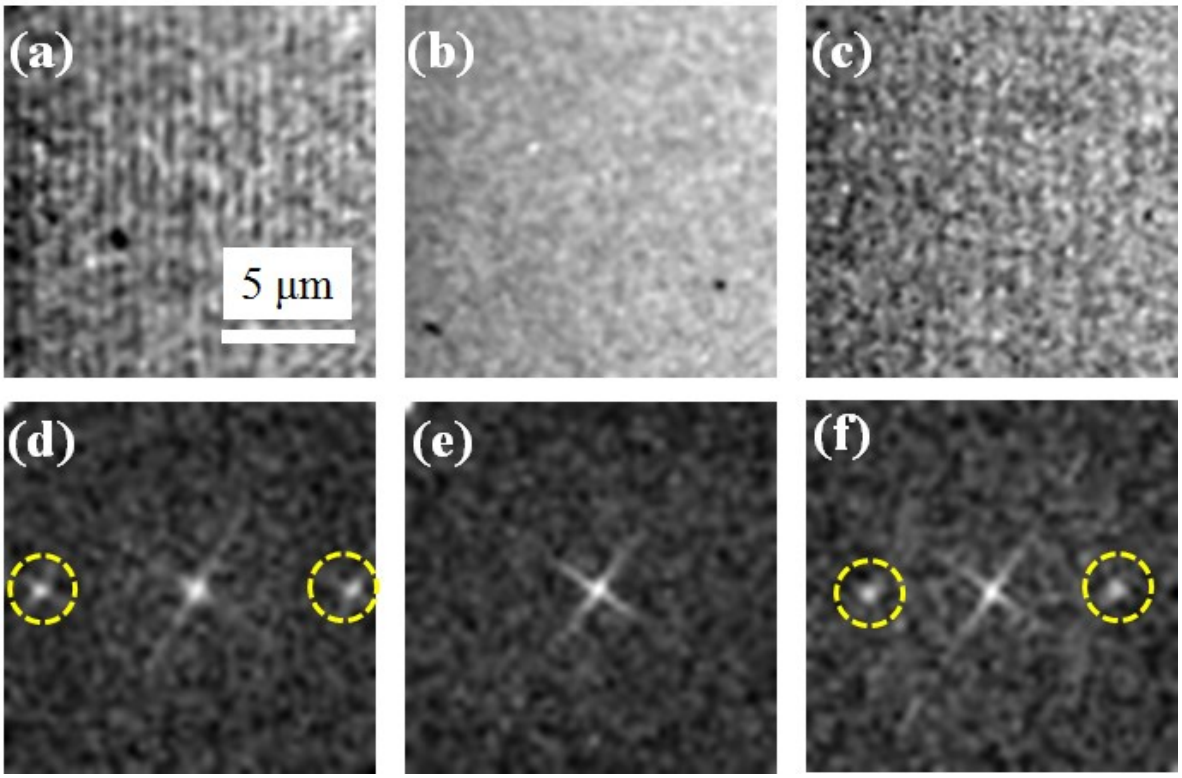

Figure S1 | Lorentz imaging at different focus modes. Lorentz images of the transient magnetic grating at **(a)** under-focus (-5 mm), **(b)** in-focus (0 mm), and **(c)** over-focus (+5 mm). A contrast reversal is observed between Fig S1(a) and Fig S1(c). The results were recorded under an external magnetic field $\mu_0 H_{ext}$ = 250 mT and by applying sample tilt angles $\alpha = 3^0$ and $\beta = 0^0$. **(d-f)** FFTs of the micrographs in **(a-c)**. The yellow dashed circles in (d) and (f) indicate the relevant periodicity for the transient magnetic grating.

Supplementary Note 2 | Formation of the Transient Optical Grating

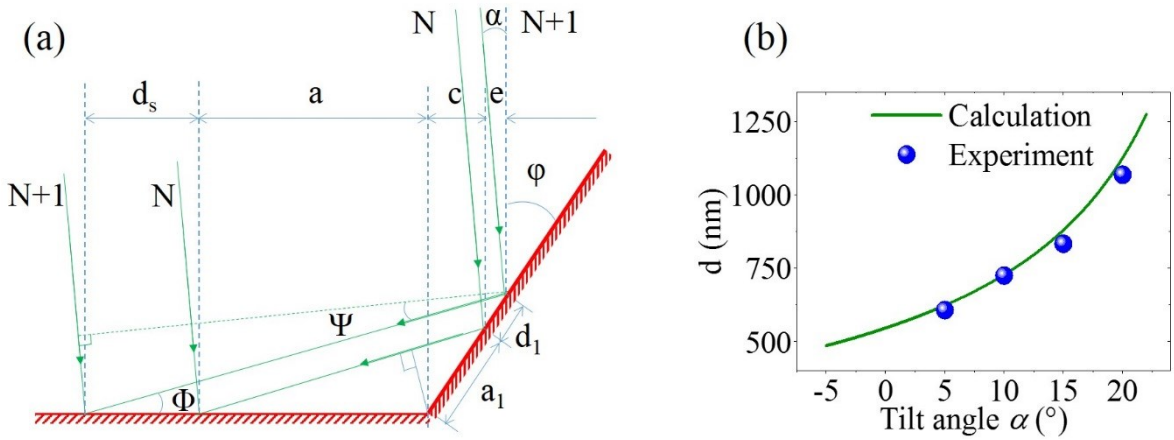

Figure S2 | (a) Optical geometry relevant for the formation of a transient optical grating at the sample. All parameters in the figure are defined in the text below. **(b) Calculated and experiment results of the periodicity, d, for the optical grating.**

Careful alignment of the pump laser beam to the edge of the electron transparent membrane grid will split the laser beam into two paths. The direct laser beam and the beam reflected from the slanted side face of the membrane window will interfere at the membrane sample plane. The condition for constructive wave interference determines the spatial period of the transient optical grating. The incident laser beams, marked as green arrows, are parallel. The reflecting slanted side face and the thin film sample plane are marked in red. Relevant geometrical parameters are defined in Fig. S2. By applying the conditions for constructive interference and phase shift upon reflection we can formulate an expression for the optical path difference between the direct and reflected beams for the *N* order (b_N):

$$b_N = \left(N + \frac{1}{2}\right) \cdot \lambda = \frac{(a + c)}{cos(\Phi)} \cdot (1 - sin(\Psi)) \qquad \text{(S1)}$$

The equivalent expression for the *N+1* order:

$$b_{N+1} = \left(N + 1 + \frac{1}{2}\right) \cdot \lambda = \frac{(d_s + a + c + e)}{cos(\Phi)} \cdot (1 - sin(\Psi)) \qquad \text{(S2)}$$

$$b_{N+1} - b_N = \lambda = \frac{(d_s + a + c + e)}{cos(\Phi)} \cdot (1 - sin(\Psi)) - \frac{(a + c)}{cos(\Phi)} \cdot (1 - sin(\Psi)) \qquad \text{(S3)}$$

Which means

$$(d_s + a + c + e) - (a + c) = d_s + e = \frac{\lambda cos(\Phi)}{1 - sin(\Psi)} \qquad \text{(S4)}$$

Where $\Phi = \pi/2 - 2\varphi + \alpha$, $\Psi = \pi/2 - 2\varphi - 2\alpha$, and $\varphi = 35^0$, and α is defined as the sample tilt angle around the X axis. From geometrical considerations we find:

$$\frac{d_s}{d_1} = \frac{a}{a_1} = \frac{d_s}{e/sin(\varphi)} \tag{S5}$$

And

$$a \cdot \sin(\Phi) = a_1 \cdot sin(\varphi + \alpha) \tag{S6}$$

$$e = \frac{sin(\Phi)sin(\varphi)}{sin(\varphi + \alpha)} \cdot d_s \tag{S7}$$

As shown in Fig. S2, d_s is the distance between the N and N+1 order beams, which is the spatial periodicity of the interference fringes at the sample plane. As the sample is tilted by an angle α, the spatial periodicity of the transient optical grating d at the detector plane is the projection of d_s onto the detector plane:

$$d = d_s \cdot cos(\alpha) \tag{S8}$$

Combining Eq. S4 , Eq. S7 and Eq. S8 results the following expression:

$$d = \frac{\dfrac{\lambda \cdot sin(2\varphi + \alpha)cos(\alpha)}{1 - cos(2\varphi + 2\alpha)}}{1 + \dfrac{cos(2\varphi + \alpha)sin(\varphi)}{sin(\varphi + \alpha)}} \tag{S9}$$

Supplementary Note 3 | Transient Magnetic Contrast at Different Laser Wavelength

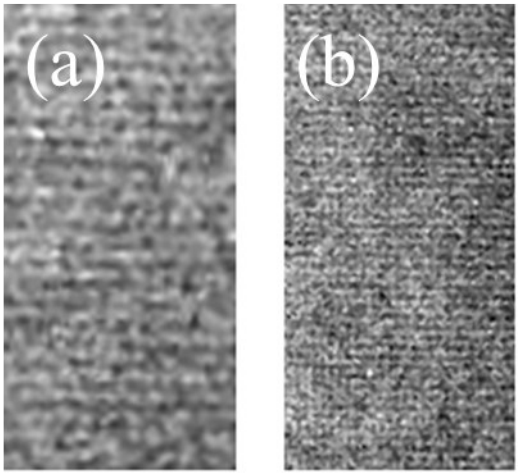

Figure S3 | (a-b) Comparison of Lorentz UEM images from transient magnetic contrast formed from excitation by transient optical gratings using laser wavelengths of λ= 1030 nm **(a)** and λ= 515 nm **(b)** with the same tilt angle $\alpha = 3^0$, $\beta = 0^0$. The dimensions of two images are both 28 μm × 14 μm. The spatial periodicity d_{IR} = 1180 nm in **(a)** is twice the periodicity d_{GREEN} = 590 nm in **(b)**.

Supplementary Note 4 | Time dependent local sample temperature

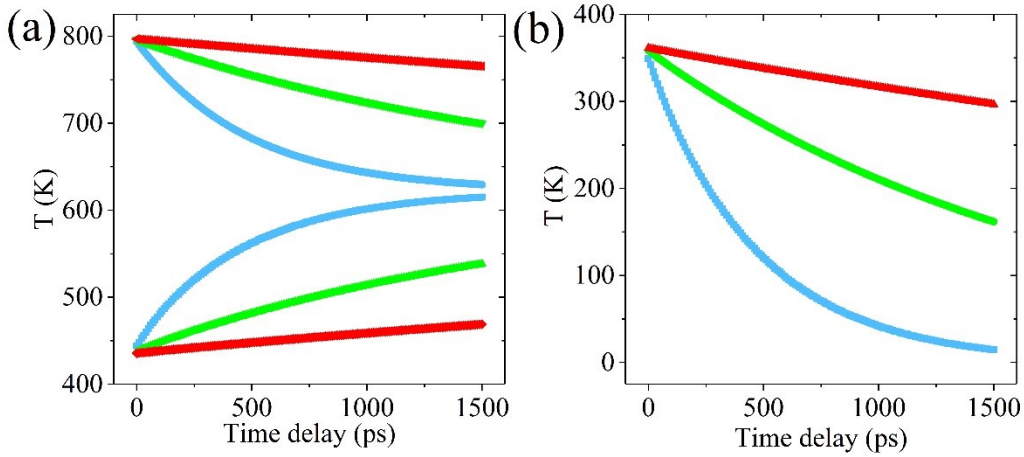

Figure S4 | (a) Calculated time dependent local temperatures in sample regions of constructive (upper curves) and destructive (lower curves) interference of the transient optical grating at laser wavelengths λ= 248 nm (blue), λ= 515 nm (green), and λ= 1030 nm (red) with the same tilt angle $\alpha = 3^0$, $\beta = 0^0$. **(b)** Corresponding temperature differences between constructive and destructive regions in **(a)**.

The following assumptions were used in the simulations of the time dependent local temperatures shown in Fig. 5(a) in the main text and Fig. S4. The initial spatial temperature distribution (immediately following photoexcitation) shown in Fig. 3h of the main text was used as an initial condition for the simulations. We use periodic boundary conditions with a spatial periodicity d determined according to Supplementary Note 2. For excitation at a laser wavelength λ = 515 nm and a tilt angle $\alpha = 3^0$, $\beta = 0^0$, we arrive at a periodicity of the thermal grating d = 590 nm. The thermal diffusivity of $Ni_{80}Fe_{20}$ is α_0 = 8.7 mm^2/s (45). The time dependent temperature distribution was obtained by solving the one-dimensional heat equation (S10):

$$\partial T/\partial t = \alpha_0 \nabla^2 T \qquad \text{(S10)}$$

Fig. S4(a) shows the time dependent local temperature in sample regions of constructive (upper curves) and destructive (lower curves) interference of the transient optical grating at laser wavelengths λ = 248 nm (blue), λ = 515 nm (green), and λ = 1030 nm (red). Fig. S4(b) shows the corresponding temperature differences between constructive and destructive regions in Fig. S4(a).

Supplementary Note 5 | Analysis of Oscillating Magnetic Moments

In this note, we describe the Lorentz contrast mechanism of the magnetic precession induced by the transient optical grating. The experimental conditions are adapted from Fig. 5(d) in the main text.

The local sample temperature, *T,* is assumed to be linearly dependent on the local laser fluence:

$$T = a_T + T_{rise} + \Delta T = a_T + b_T \cdot F + c_T \cdot F_L, \tag{S11}$$

where a_T = 293 K is the sample temperature with no pump laser. $T_{rise} = b_T \cdot F$, represents the temperature increase of the sample region at negative time delays due to the lingering optical power absorbed in the pump region of the sample during pump-probe analysis. T_{rise} may be estimated from applying Weiss molecular field theory to the decrease in magnetic Lorentz contrast at negative time delays from a magnetic vortex grown on a similar TEM grid (27). From considering a similar sample geometry as in reference (27) and the repetition rate used in the present experiments (35 kHz), b_{T} can be estimated to approximately 4 K·cm^2/mJ. A laser fluence of F = 9 mJ/cm^2 will then result in a T_{rise} of approximately 36 K. The term $\Delta T = c_T \cdot F_L$ corresponds to the rapid local temperature increase of the lattice after the recombination of the photoexcited electronic carriers (a few ps after photoexcitation (46)). F_L is the local laser fluence on the sample that is spatially periodic due to the nature of the transient optical grating. c_T is determined from sample-specific parameters: thickness, density, absorption coefficient, and heat capacity. The absorption coefficient of $Ni_{80}Fe_{20}$ at 515 nm is approximately 50% (from reflectivity measurements), the density ρ = 8.90 g/cm^3, the heat capacity c_p = 0.445 J/g·K (45), and the sample thickness 50 nm. Taken together this results in c_{T} = 25.2 K·cm^2/mJ, or a local temperature jump ΔT = 25.2 K for a local laser fluence of F = 1 mJ/cm^2.

After confirmed the temperature dependence of fluence on the sample, the magnetization $M(T)$ can be derived as a function of the temperature T, which can be described by the Weiss molecular field theory (37):

$$M(T) = M_S \cdot tanh[\frac{T_C M(T)}{T \quad M_S}], \tag{S12}$$

where $\mu_0 M_{\mathrm{s}}$ = 0.98 T is the saturation magnetization of permalloy at room temperature (38) and T_{c} = 871 K is the Curie temperature of permalloy (33).

Excitation via a transient optical grating results in a spatially periodic local laser fluence on the sample. The local temperature is directly coupled to the local fluence at short time delays. The local temperature at longer delays will be governed by thermal diffusion as reported in Fig. 5(a) of the main text and in Supplementary Note 4. The time dependent local magnetization $M(T)$ is correlated with the local temperature (Eq. S12).

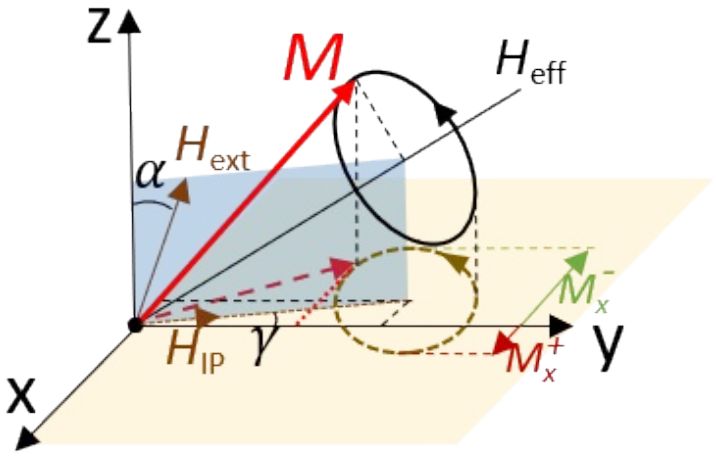

Figure S5 | Schematic illustration of the precession of the magnetic moments. The black solid circle traces the precession of the local magnetic moment (M) around the effective magnetization direction ($\boldsymbol{H}_{\text{eff}}$). The dashed circle shows the projection of the precession onto the xy plane. $\boldsymbol{H}_{\text{ext}}$ indicates the applied magnetic field, α is the angle of the applied field relative to the sample normal, the red dashed arrow is the projection of $\boldsymbol{H}_{\text{ext}}$ in x-y plane, i. e. $\boldsymbol{H}_{\text{IP}}$. γ is the angle between $\boldsymbol{H}_{\text{IP}}$ and Y axis.

The ultrafast laser-induced demagnetization induces a change in the equilibrium direction of the magnetization ($^{H_{eff}}$) immediately, shown in Fig. S5. $^{H_{eff}}$ can be determined from: (33,38)

$$\begin{cases} H_{ext} \cdot \sin(\alpha) = H_{eff} \cdot \sin(\theta_{eff}) \\ H_{ext} \cdot \cos(\alpha) = [H_{eff} + M(t)] \cdot \cos(\theta_{eff}) \end{cases}, \tag{S13}$$

where the external field $\mu_0 H_{ext} = 0.25$ T and the angle of the external field relative to the sample normal $\alpha = 3°$. $^{H_{eff}}$ and $^{\theta_{eff}}$ is the equilibrium field and angle, respectively. Before laser excitation, $\mu_0 M = 0.97T$ at $T = a_T + T_{rise} = 333$K and the calibrated equilibrium angle $\theta_{eff}^{RT} = 17^{\circ}$. The laser-induced ultrafast demagnetization change the equilibrium direction with a new angle $\theta_{eff}^{T}(t)$. This makes the magnetization precession around this new equilibrium direction. The temporal precession angle $\theta^T(t)$ is therefore:

$$\theta^T(t) = \theta_{eff}^{T}(t) - \theta_{eff}^{RT}. \tag{S14}$$

The precession angle is influenced by two mechanisms: 1) a change in the effective field direction; 2) Due to the damping of permalloy, the precession angle drags the magnetization to the effective field direction. This allows us to formulate expressions of time dependent precession angle

$$\theta(t) = \theta^T(t) \cdot \theta^{\alpha_{eff}}(t) = \theta^T(t) \cdot e^{-2\pi\alpha_{eff} \cdot t}. \tag{S15}$$

The second term is related to the effective damping contribution. We use the effective damping parameter (α_{eff} = 0.008) in the simulations (47). f is the precession frequency, which can be calculated based on the modified Kittel equation with exchange coupling field: (40)

$$f = \frac{\gamma_G}{2\pi}\mu_0\sqrt{(H_{eff} + H_{ex})[H_{eff} + H_{ex} + M \cdot cos^2(\theta_{eff})]} \tag{S16}$$

where $\frac{\gamma_G}{2\pi} = 28$ GHz/T (38) is the gyromagnetic ratio, H_{ex} is the additional effective field due to the exchange coupling. μ_0 is the permeability of free space. The calculated frequency is presented in Fig. 5(b) in the main text.

The magnetization then precesses around the equilibrium center $[x_c(t),\ y(t),\ z(t)]$ with radius $r(t)$ in Fig. S5, which have the relationships

$$r(t) = M(t) \cdot sin[\theta(t)]\ , \tag{S17}$$

$$\begin{cases} x_c(t) = M(t) \cdot \cos\left[\theta_{eff}^{T}(t)\right] \cdot sin(\gamma) \\ y_c(t) = M(t) \cdot \cos\left[\theta_{eff}^{T}(t)\right] \cdot cos(\gamma) \\ z_c(t) = M(t) \cdot \sin\left[\theta_{eff}^{T}(t)\right] \end{cases}, \tag{S18}$$

Then the *x* component of magnetization $M_x(t)$ is derived as

$$M_x(t) = x_c(t) + r(t)\left\{\frac{y_c(t)}{\sqrt{[y_c(t)]^2 + [y_c(t)]^2}}cos[2\pi f(t - t_0)] + \frac{x_c(t) \cdot z_c(t)}{\sqrt{[x_c(t) \cdot z_c(t)]^2 + [y_c(t) \cdot z_c(t)]^2 + \left([y_c(t)]^2 + [y_c(t)]^2\right)^2}}cos[2\pi f\right. \tag{S19}$$

Here we consider representative regions at constructive (maximum) and deconstructive (minimum) interference of the transient optical grating to calculate the time dependent maximum $M_x^{max}(t)$ and minimum $M_x^{min}(t)$ local magnetization. The time dependent Lorentz contrast is related to the absolute difference between $M_x^{max}(t)$ and $M_x^{min}(t)$,

$$\Delta M_x(t) = \left|M_x^{max}(t) - M_x^{min}(t)\right|. \tag{S20}$$

The detected Lorentz contrast is linearly dependent $\Delta M_x(t)$ (48):

$$c_{Lorentz}(t) = c_{Lorentz} \cdot \Delta M_x(t) \tag{S21}$$

where c_{Lorentz} represents a proportionality constant for the Lorentz contrast.

A deviation of the applied in-plane magnetic field component from the Y direction (rotation by angle γ) results in an asymmetric modulation of $M_x(t)$ at different phases of the precession. Under conditions with a precession angle of $\theta = 17^0$ and $0 < \gamma < \theta$ the ratio between the first (phase $\pi/2$) and second peak (phase $3\pi/2$) in the temporal FFT intensity trace of the periodic magnetic Lorentz contrast is modulated as follows,

$$\frac{M_{X,max}^{+}}{M_{X,max}^{-}} = \frac{sin(\theta+\gamma)}{sin(\theta-\gamma)} \tag{S22}$$

Under conditions with $\theta \leqslant \gamma < \pi/2$, the M_X projection will no longer change sign during the precession and no reversal of Lorentz contrast is detected. This implies that peaks at precession phases $3\pi/2 + n*2\pi$ (n = 0, 1, 2…) will be suppressed in the temporal FFT intensity trace of the magnetic Lorentz contrast and $M_{x,max}+$ may be calculated from the following expression:

$$M_{X,max}^{+} = M \cdot sin(\theta+\gamma) \tag{S23}$$

Supplementary Note 6 | Lorentz image simulation using OOMMF & MALTS

We use the Object Oriented MicroMagnetic computing Framework (OOMMF) (49) to construct the local spin configuration of four illustrative phases during the magnetic precession (0, $\pi/2$, π, and $3\pi/2$). Since the sample thickness is limited (50 nm) and permalloy exhibits in-plane magnetization anisotropy, the spin configuration of the sample may be treated in a 2D model. However, as the exciting transient optical grating is uniform along the X-axis of the sample, the 2D spin configuration can be simplified to a 1D spin configuration. The spin configuration is periodic along the X-axis direction of the sample, with the same periodicity as the exciting transient optical grating. The magnetic moment of each cell is defined by the local magnetization vectors M_X and M_Y. M_X and M_Y are extracted for each cell from the calculations presented in Supplement Note 5. The resulting magnetization matrix serves as input to the spin configuration file. After generating the spin configuration by OOMMF, we employ the Micromagnetic Analysis to Lorentz TEM Simulation (MALTS) (50) software to simulate the Fresnel mode LTEM (Lorentz Transmission Electron Microscopy) contrast images from the OOMMF spin configuration. The resulting simulations are shown in Fig. 4(d) and (h) of the main text.